Toward Spectral-domain Optical Coherence Tomography on a Silicon Chip

B. I. Akca[1], B. Považay[2], A. Alex[2], K. Wörhoff[1], R. M. de Ridder[1], W. Drexler[2], and M. Pollnau[1]

[1]*Integrated Optical MicroSystems Group, MESA+ Institute for Nanotechnology, University of Twente, Enschede, The Netherlands.*

[2] *Center for Medical Physics and Biomedical Engineering, Medical University of Vienna, Austria.*

e-mail: imran.akca@gmail.com

Abstract: *In-vivo* imaging was demonstrated with a depth range of 1.4 mm and axial resolution of 7.5 µm by using a miniaturized spectral-domain optical coherence tomography system comprising an on-chip integrated spectrometer and beam splitter.

OCIS codes: (170.4500) Optical coherence tomography; (230.3120) Integrated optics devices

1. Introduction

Optical coherence tomography (OCT) is a well-established optical technique in the medical sciences for acquiring micrometer-scale-resolution cross-sectional images of specimen in a non-invasive way [1]. Current OCT systems contain a variety of fiber and free-space optical components, which add to the instrument size and cost. Besides, the imaging quality is sensitive to the correct alignment of each individual element. In order to make these instruments more readily accessible, compact, significantly cheaper, and maintenance-free OCT systems are demanded. By utilizing a suitable mass-fabrication technology and a monolithic design, integrated optics can provide miniaturized OCT systems that offer dramatic cost and size reduction as well as more stable interferometric detection [2-5].

In this paper we present an important step toward a cheap, compact, and quasi-maintenance-free spectral-domain OCT (SD-OCT) system by integrating its central components, the beam splitter and spectrometer, on a silicon chip as schematically shown in Fig. 1. An arrayed waveguide grating (AWG) [6] operating at a center wavelength of 1250 nm (ideal for skin imaging) with a large free spectral range of 136 nm and a high wavelength resolution (Δλ) of 0.21 nm forms the integrated spectrometer, and a non-uniform adiabatic coupler [7] forms the beam splitter in our device. *In-vivo* imaging with the partially integrated SD-OCT system is demonstrated in human skin with a depth range of 1.4 mm, axial resolution of 7.5 µm, and signal-to-noise ratio (SNR) of 74 dB. For comparison, utilizing the same light source, detection system, patient interface, sample, and processing method OCT images are taken with a 1300 nm fiber-based, custom-designed SD-OCT system.

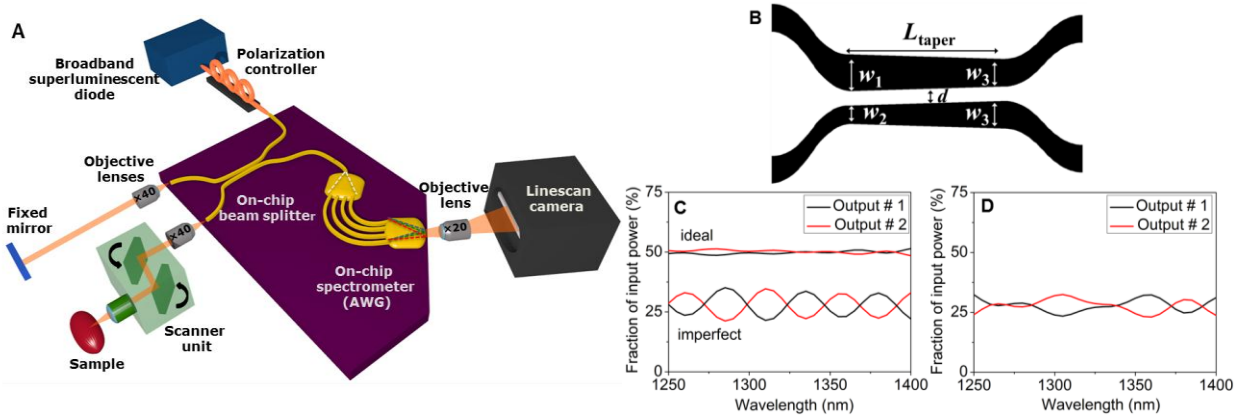

Fig.1. Schematic of (*A*) the partially-integrated SD-OCT system with an on-chip beam splitter (BS) and an arrayed-waveguide grating (AWG) spectrometer. (*B*) 3-dB non-uniform adiabatic coupler which forms the on-chip BS. (*C*) Simulation result of the non-uniform adiabatic coupler in the ideal case, i.e., without any fabrication imperfection (curve "ideal'), and including incomplete etching of the SiON layer in the gap region (curves "imperfect"). (*D*) Optical transmission measurement result of the fabricated non-uniform adiabatic coupler.

2. Design

Non-uniform adiabatic coupler design: We designed a linearly tapered directional coupler [7] to have a very weak wavelength dependence over a range larger than 150 nm. The schematic of the non-uniform adiabatic coupler is illustrated in Fig. 1*B*. In the straight section of the coupler, the waveguides were tapered from w_1 = 2 µm down to w_3 = 1.8 µm and from w_2 = 1.6 µm up to w_3 = 1.8 µm, respectively, over a length of L_{taper} = 3.5 mm. The gap between waveguides was chosen as d = 0.8 µm. The coupler was simulated using the beam propagation method and a

constant 3-dB splitting ratio was achieved over 150 nm wavelength range as given in Fig. 1*C*. The fabricated coupler showed a coupling ratio exhibiting an oscillatory wavelength dependence with a splitting ratio of ± 1.76 dB, and 2.5 dB excess loss (Fig. 1*D*), which could be largely explained by a fabrication error. Simulation of the unintended incomplete etching of the waveguide core layer in the gap between the waveguides produced a qualitative agreement with the measurements (labeled as 'imperfect' in Fig. 1*C*). The waveguides at the air/SiON interface were tapered from 1.8 μm to 3 μm in order to increase the back-coupled light efficiency. Unfortunately, an unexpected destructive wavelength-dependent interference was observed in the spectrum due to these tapered sections, which reduced the usable spectrum down to 75 nm.

AWG design: For this device, we aimed at 7.5-μm depth resolution (determined by the full width at half maximum values of the transmission spectrum of the AWG) and 2-mm depth range (determined by the wavelength resolution). In conventional AWGs the wavelength resolution is limited by the number of output channels. By omitting these channels and imaging the AWG's output focal plane directly onto a camera, the resolution will be determined by the diffraction limit due to the dimensions of the AWG's second free propagation region and by the number of camera pixels. In this way, the depth range can be significantly increased. In order to image the light onto the entire detector array (1024 pixels), the magnification of the objective lens was arranged to be ×10. The overall spectral resolution was calculated as 0.21 nm [8], which results in an improved depth range of 2 mm in air compared to only 0.5 mm with output channels.

Single-mode silicon oxynitride (SiON) channel waveguides with 2 μm width and 0.8 μm height were used for the AWG spectrometer as well as for the beam splitter. For the upper cladding 4-μm-thick silicon dioxide was used. The core and cladding refractive indices were 1.54 and 1.4485 at 1.3 μm, respectively. The minimum bending radius of curved waveguides was calculated to be 500 μm.

3. Measurements and Results

The AWG spectrometer and the tapered coupler were integrated on a chip, which was interfaced to the light source, an external reference arm, a 2-dimensional scanning system, and a linescan camera, as indicated in Fig. 1*A*. A Labview programming interface (National Instruments) was employed for detection, control and real-time display. The *k*-mapping and the dispersion-compensating procedures were previously explained in detail [9]. As a demonstration of the feasibility of OCT on a chip, *in vivo* imaging of human skin was performed above the proximal interphalangeal joint of the middle finger by applying contact gel to the imaging sites as an index-matching medium to decrease the surface reflectivity. The averaged *en face* and the corresponding cross-sectional tomogram of the proximal interphalangeal joint of the middle finger are given in Fig. 2*A*-*D*, with corresponding regions indicated by colored marks or the dashed lines, respectively. The morphology of several layers including the stratum corneum and living layers of the epidermis (Fig. 2*A*), the stratum papillare and reticulare of the dermis (Fig. 2*B*), and the deeper dermis featuring vessels (Fig. 2*C*) has been visualized within a depth range of 1.4 mm.

The imaging performance of the on-chip SD-OCT system was compared to a 1300 nm fiber-based custom-designed SD-OCT system [10] by acquiring OCT images of scar tissue utilizing the same patient interface, light source, detection system, and processing method. The axial resolution of the custom-designed SD-OCT system was obtained as ~5.7 μm in tissue, which is slightly better than the 7.5 μm resolution of the partially integrated SD-OCT system. However, the 74-dB-SNR of the partially integrated SD-OCT system lags behind the 94-dB-value of the custom-made SD-OCT system. Figure 2*E* shows the OCT image taken with 32x averages using the 1300 nm fiber-based custom-designed SD-OCT system. The zero delay of the partially integrated SD-OCT system was offset by ~800 μm towards the region of interest to compensate for ~10 dB loss caused by signal roll-off. The resulting OCT image, also 32x averaged, is demonstrated in Fig. 2*F*. The signal roll-off curves of the partially integrated OCT system using an AWG spectrometer and the custom-designed OCT system using a bulky spectrometer are indicated in Fig. 2*G* by the blue dashed line and black solid line, respectively. The resulting signal roll-off of the partially integrated OCT system after compensation, i.e., shifting its zero delay by ~800 μm and averaging of 32 frames, becomes close to the signal roll-off of the custom-designed OCT system, as indicated by the blue solid line in Fig. 2*G*. Fortunately, the current implementation can be exploited further to increase the SNR of the on-chip OCT system up to 95 dB by reducing i) the non-adiabatic coupler loss close to its theoretical value of 0 dB with an optimized lithography and etching procedure, ii) fiber-to-chip coupling losses down to <0.5 dB with a tapered input waveguide (11), iii) transmission loss of the objective lens down to <1 dB with a proper objective lens designed specifically for the near-infrared range, and iv) AWG excess loss down to <0.5 dB by applying vertical tapers at the interfaces of the arrayed waveguides with the free-propagation regions [12].

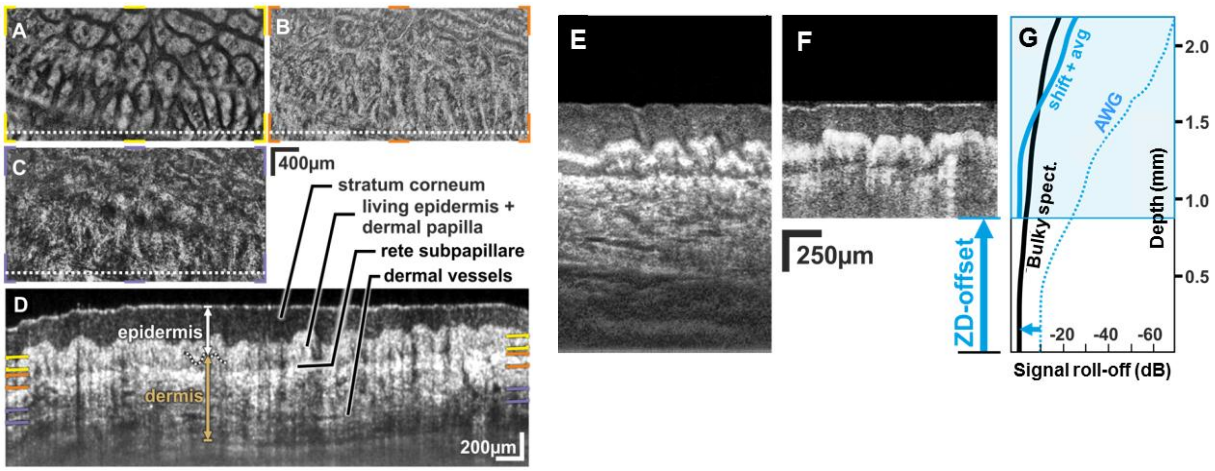

Fig. 2. Images of glabrous skin at interdigital joint taken using the partially integrated SD-OCT system: *En face* section at the (*A*, yellow) deeper epidermal layers featuring the living epidermis on top of the dermal papillae, (*B*, orange) rete subpapillare where fibrous components dominate the basis of the dermal papillae, and (*C*, violet) the deeper dermis with vessels. (*D*) Cross-section as indicated by the dotted white line in the *en face* sections. Colored indicators depict the location of the *en face* views. Cross-sectional tomograms of the scar tissue at the index finger taken with 32× average using (*E*) the 1300-nm custom-designed SD-OCT system, and (*F*) the partially integrated SD-OCT system. (*G*) The signal roll-off curves of the partially integrated OCT system using an AWG spectrometer and the custom-designed OCT system using a bulky spectrometer are indicated by the blue dashed line and black solid line, respectively. The resulting signal roll-off of the partially integrated OCT system after compensation is given by the blue solid line in (*G*).

4. Conclusions

In conclusion, *in vivo* imaging with a partially integrated SD-OCT system has been demonstrated by acquiring volumetric images of human skin in multiple locations and subjects. An in-tissue axial resolution of 7.5 µm and in-tissue depth range of 1.4 mm was achieved. The performance of the current partially integrated OCT system can be further improved to the level of bulky commercial OCT systems with an optimized design and high-quality fabrication facilities.

This work was financially supported by the Smart Mix Program of the Netherlands Ministry of Economic Affairs and the Netherlands Ministry of Education, Culture and Science and the Medical University Vienna, European Union project FUN OCT (FP7 HEALTH, contract no. 201880).

5. References

[1] D.Huang, E. A. Swanson, C. P. Lin, J. S. Schuman, W. G. Stinson, W. Chang, M. R. Hee, T. Flotte, K. Gregory, C. A. Puliafito, and J. G. Fujimoto, "Optical coherence tomography," Science 254, 1178–1181(1991).

[2] D. Choi, H. Hiro-Oka, H. Furukawa, R. Yoshimura, M. Nakanishi, K. Shimizu, and K. Ohbayashi, "Fourier domain optical coherence tomography using optical demultiplexers imaging at 60,000,000 lines/s," Opt. Lett. 33, 1318–1320 (2008).

[3] V. D. Nguyen, N. Weiss, W. Beeker, M. Hoekman, A. Leinse, R. G. Heideman, T. G. van Leeuwen, and J. Kalkman, "Integrated-optics-based swept-source optical coherence tomography," Opt. Lett. 37, 4820–2822 (2012).

[4] B. I. Akca, V.D. Nguyen, J. Kalkman, N. Ismail, G. Sengo, F. Sun, T. G. van Leeuwen, A. Driessen, M. Pollnau, K. Wörhoff, and R. M. de Ridder, "Toward spectral-domain optical coherence tomography on a chip," IEEE J. Sel. Top. Quantum Electron. 18,1223–1233 (2012).

[5] I. B. Akca, L. Chang, G. Sengo, K. Wörhoff , R. M. de Ridder, and M. Pollnau, "Polarization-independent enhanced-resolution arrayed-waveguide grating used in spectral-domain optical low-coherence reflectometry," IEEE Photon. Technol. Lett. 24, 848–850 (2012).

[6] M. K. Smit, "New focusing and dispersive planar component based on an optical phased array," Electron. Lett. 24, 385–386 (1988).

[7] W. H. Louisell, "Analysis of the single tapered mode coupler," The Bell Syst. Tech. J. 33, 853–870 (1955).

[8] Z. Hu, Y. Pan, and A. M. Rollins, "Analytical model of spectrometer-based two-beam spectral interferometry," Appl. Opt. 46, 8499–8505 (2007).

[9] B. Hofer, B. Povazay, B. Hermann, A. Unterhuber, G. Matz, W. Drexler, "Dispersion encoded full range frequency domain optical coherence tomography," Opt. Express 17, 7–24 (2009).

[10] A. Alex, B. Povazay, B. Hofer, S. Popov, C. Glittenberg, S. Binder, and W. Drexler, "Multispectral in vivo three-dimensional optical coherence tomography of human skin," J. Biomed. Opt. 15, 026025(1–14) (2010).

[11] O. Mitomi, K. Kasaya, and H. Miyazawa, "Design of a single-mode tapered waveguide for low-loss chip-to-fiber coupling," IEEE J. Quantum Electron. 30, 1787–1793 (1999).

[12] A. Sugita, A. Kaneko, K. Okamoto, M. Itoh, A. Himeno, and Y. Ohmori, "Very low insertion loss arrayed-waveguide grating with vertically tapered waveguides," IEEE Photon. Technol. Lett. 12, 1180–1182 (2000).